ORGANIC CHEMISTRY

Trifluoromethylation of alkyl electrophiles with ^{11}C- or ^{18}F-labeled fluoroform for PET applications

Chao Wang[1,2,3]†, Paul DeMent[2]†, Susovan Jana[2], Jinsoo Hong[2], Victor W. Pike[2]*, Wei Liu[1,3]*

Continued development of positron emission tomography (PET) tracers is essential for advancing molecular imaging in biomedical research and clinical diagnostics. A long-standing limitation in radiochemistry for PET imaging has been the lack of general methods for radiolabeling trifluoromethyl (CF_3) groups at C(sp^3) sites, despite their growing prevalence in bioactive molecules and radiopharmaceuticals. Here, we present a general approach for late-stage installation of either a [^{18}F]CF_3 or [^{11}C]CF_3 group at a C(sp^3) site. This method leverages unusual copper-mediated radiotrifluoromethylation of alkyl halides and alkyl carboxylic acids by halogen atom transfer and photoredox catalysis, respectively. More than 50 complex molecules and pharmaceutical agents were efficiently labeled with fluorine-18 (^{18}F) or carbon-11 (^{11}C). Two long-sought-after radioligands, [^{18}F]SL25.1188 and [^{18}F]PS13, were synthesized, providing longer-lived ^{18}F analogs of their ^{11}C counterparts with great promise for human PET imaging.

Positron emission tomography (PET) with a broad range of tracers has become an indispensable tool in modern medical diagnosis and research (*1*–*4*). This molecular imaging technique has burgeoning importance for biomedical research, drug development, disease diagnosis, and therapy monitoring. The development of PET imaging relies heavily on the continuous innovation of new tracers to expand the range of biochemical measurements. These tracers are typically organic molecules labeled with positron-emitting radionuclides (*5*, *6*). Among these, carbon-11 (^{11}C) and fluorine-18 (^{18}F) are the most widely used owing to their ease of cyclotron production, suitable half-lives (^{11}C $t_{1/2}$ = 20.4 min; ^{18}F $t_{1/2}$ = 109.8 min), and capacity for covalent incorporation into tracer molecules. Despite advances in carbon-11 chemistry (*5*–*9*) and fluorine-18 chemistry (*10*–*20*), PET tracer development and regular production (*21*) are mainly confined to two labeling strategies: ^{11}C-methylation of *O*- or *N*-based nucleophiles (*22*) and nucleophilic ^{18}F-fluorination of alkyl and aryl electrophiles. Consequently, many molecular structures have remained challenging to radiolabel and transform into PET tracers, hindering the full potential of this technology.

A critical challenge in PET tracer development is the lack of a universally applicable method for introducing radiolabeled trifluoromethyl (CF_3) groups at unactivated C(sp^3) sites (Fig. 1A). The desire to install CF_3 groups in radiopharmaceuticals stems from the growing prevalence of alkyl-CF_3 moieties in bioactive molecules (*23*) and their impact on drug metabolism, stability, and lipophilicity (*24*–*26*). Moreover, owing to the higher bond dissociation energy (BDE) of C–F bonds in CF_3 groups (BDE = ~128 kcal/mol) than in CH_2F groups (BDE = ~110 kcal/mol), alkyl-[^{18}F]CF_3 molecules could potentially serve as superior analogs of the corresponding alkyl-^{18}F PET probes, many of which suffer from metabolic defluorination (*27*, *28*). Finally, the ability to install either a carbon-11 or fluorine-18 label in the same compound offers an expanded opportunity for investigating new PET tracers: The short half-life of carbon-11 enables multiple tracer scans on the same subject in a single day and thus rapid local clinical studies, whereas the longer half-life of fluorine-18 allows the distribution of tracers from a central cyclotron facility. Thus, accessing both ^{11}C- and ^{18}F-labeled molecules with complementary imaging utilities from a single precursor through a unified strategy represents a useful avenue for PET tracer development.

The integration of radiolabeled C(sp^3)–CF_3 groups into organic structures remains a synthetic hurdle. Although aromatic radiotrifluoromethylation reactions have been reported (*29*), methods for incorporating radiolabeled CF_3 groups at C(sp^3) centers are rare and largely limited to specific chemical structures (*30*–*32*). Existing strategies, such as nucleophilic substitution of difluoromethylene precursors (RCF_2X) with [^{18}F]fluoride or the nucleophilic addition to geminal difluorovinyl complexes ($RCH{=}CF_2$) (*33*–*39*), suffer from limited scope, suboptimal radiochemical yields, and difficulties in precursor synthesis (*40*). Additionally, the fluoride-rebound approach developed by Toste *et al.* for C(sp^3)–[^{18}F]CF_3 bond formation, although mechanistically intriguing, is hindered by low molar activity (A_m) and the intricate nature of multistep organometallic synthesis, restricting its broader applicability in PET tracer development (*41*). Consequently, the absence of an efficient and versatile method for radiolabeling C(sp^3)–CF_3 groups restricts the scope for developing new PET tracers (Fig. 1B). For example, two CF_3-containing radioligands, [^{11}C]**SL25.1188** (*42*) and [^{11}C]**PS13** (*43*), have shown high performance as PET imaging agents targeting monoamine oxidase and cyclooxygenase-1, respectively. However, the inability to efficiently radiolabel their CF_3 groups has impeded the synthesis of their highly desirable ^{18}F-analogs, which would offer much broader clinical applications because of the longer half-life of fluorine-18 than that of carbon-11.

Our group (*44*) and others (*45*, *46*) have recently shown that transition metals can catalyze the efficient transfer of fluoroalkyl groups to C(sp^3) sites via alkyl radical intermediates. We recently questioned whether this strategy could be translated to radiolabeling reactions, thereby enabling the coupling of alkyl electrophiles with radiolabeled CF_3 nucleophiles to establish a general approach for synthesizing CF_3-based radiopharmaceuticals (Fig. 1C). However, we realized that several key challenges could accompany this strategy. First, trifluoromethylation of alkyl electrophiles with nucleophilic CF_3 sources remains underdeveloped (*47*), necessitating the discovery of new pathways for CF_3 transfer. Second, given the short half-lives of fluorine-18 and carbon-11, the coupling reactions must proceed rapidly and be compatible with CF_3 sources that can be efficiently radiolabeled. Finally, because radiolabeling is typically performed in the final stage of synthesis, the coupling reactions must tolerate a broad range of sensitive functional groups. Here, we addressed all these challenges by developing two copper-mediated CF_3 transfer pathways: trifluoromethylation of alkyl iodides via halogen atom abstraction and photoredox-enabled decarboxylative trifluoromethylation of carboxylic acids. Both transformations have been successfully translated into radiotrifluoromethylation reactions using readily radiolabeled fluoroform as CF_3 sources, enabling the synthesis of a broad range of aliphatic [^{11}C]CF_3 and [^{18}F]CF_3 products. Moreover, this strategy has facilitated the efficient synthesis of a group of hitherto inaccessible PET tracer molecules targeting important biological markers (Fig. 1D).

Trifluoromethylation of alkyl iodides via aryl-radical–enabled iodine atom abstraction

We first aimed to develop a late-stage ^{11}C- and ^{18}F-trifluoromethylation of easily accessible alkyl halides. Although a few methods have been reported for converting alkyl halides into their alkyl-CF_3 counterparts, these methods require either the use of electrophilic trifluoromethylation

[1]Department of Chemistry, University of Cincinnati, Cincinnati, OH, USA. [2]Molecular Imaging Branch, National Institute of Mental Health, National Institutes of Health, Bethesda, MD, USA. [3]Department of Chemistry, Virginia Tech, Blacksburg, VA, USA. *Corresponding author. Email: pikev@mail.nih.gov (V.W.P.); liuwei@vt.edu (W.L.) †These authors contributed equally to this work.

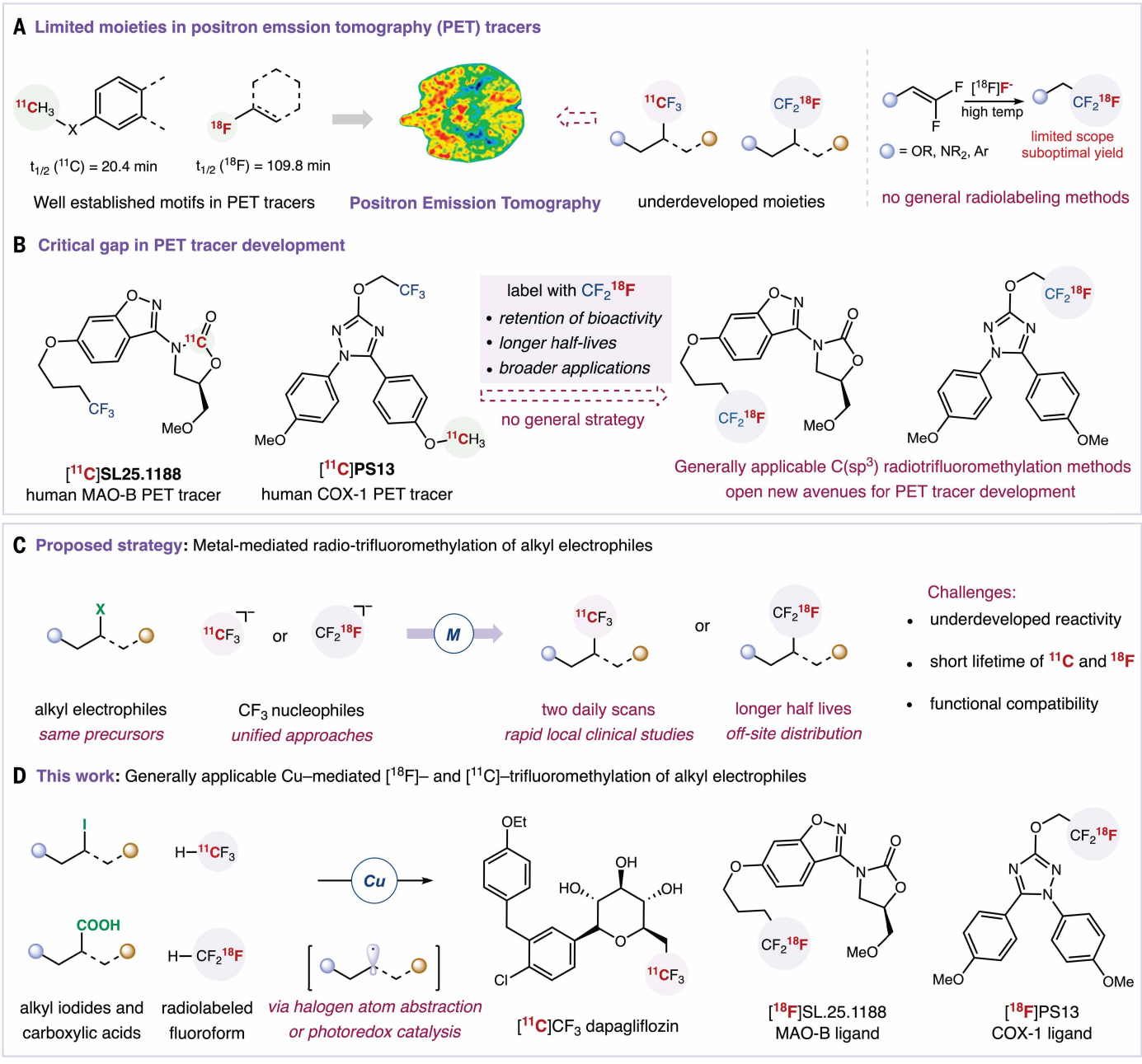

Fig. 1. Development of general approaches to ^{11}C- and ^{18}F-trifluoromethylation of alkyl electrophiles. (**A**) PET tracer development has been constrained by limited sets of labeling methods. (**B**) Advancement of PET imaging has been impacted by the lack of aliphatic radiotrifluoromethylation strategies. (**C**) Proposed general approach for transition metal–mediated ^{11}C- and ^{18}F-trifluoromethylation of alkyl electrophiles. (**D**) A generally applicable Cu-mediated ^{18}F- and ^{11}C-trifluoromethylation of alkyl iodide and alkyl carboxylic acid for the efficient synthesis of PET tracers. Ar, aryl; Et, ethyl; Me, methyl; R, substituent group.

reagents or high-valent copper reagents, which are not amenable to radiotrifluoromethylation (*45*, *47*, *48*). Recent endeavors, both from our research group (*49*, *50*) and others (*51*, *52*), have demonstrated aryl-radical–enabled iodine abstraction as a powerful platform to engage unactivated alkyl iodides in Cu-catalyzed cross-coupling reactions. These established protocols harness the marked reactivity exhibited by arenediazonium salts toward copper(I) species, coupled with swift iodine abstraction from alkyl iodides by aryl radicals. Given that these transformations take place under mild conditions and can be accomplished within 20 min, we aimed to establish a general methodology for the Cu-mediated radiotrifluoromethylation of alkyl iodides via aryl-radical–enabled iodine abstraction. It is worth noting that the hazards associated with diazonium salts are mitigated in radiochemistry because of the very small quantities required.

The feasibility of this CF_3 transfer protocol was first demonstrated through the development of a Cu-catalyzed, aryl-radical–enabled, trifluoromethylation of alkyl iodides (Fig. 2A). Thus, the use of a zinc–based CF_3 reagent, (Phen)Zn(CF_3)$_2$, where Phen is 1,10-phenanthroline, allowed for catalytic conversion of alkyl iodide **1** into the desired product **2** in 71% yield. A sterically hindered diazonium salt ($MesN_2BF_4$, where Mes is mesityl) was used to minimize the side reactions on the aryl radical. Control experiments confirmed that no desired

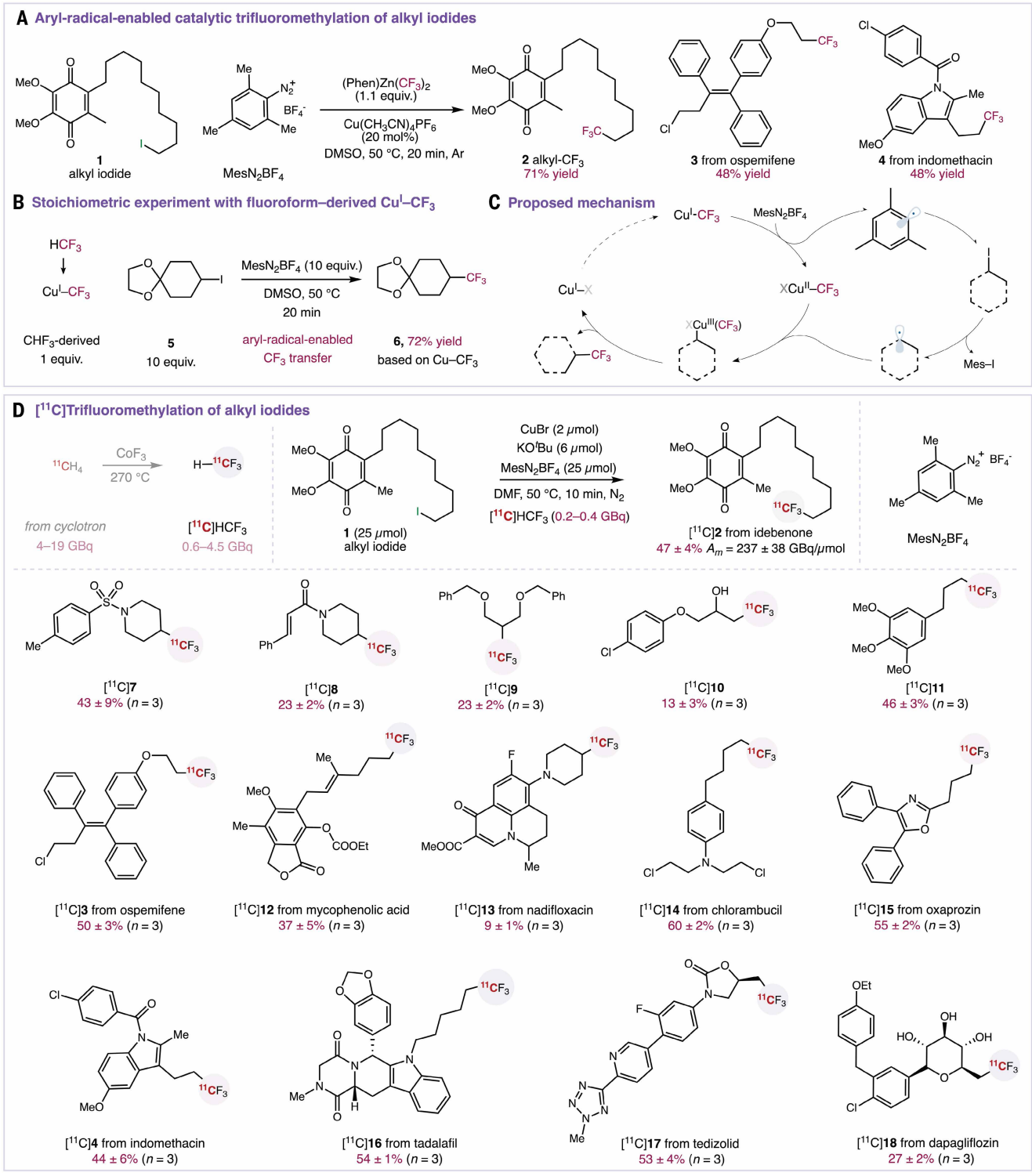

Fig. 2. ^{11}C-Trifluoromethylation of alkyl iodides. (**A**) Development of a catalytic alkyl iodide trifluoromethylation reaction (see fig. S171 for additional substrates). Isolated yields are reported. (**B**) Stoichiometric experiments with fluoroform-derived $CuCF_3$. Yield was determined by ^{19}F nuclear magnetic resonance. (**C**) Proposed mechanism for the trifluoromethylation reaction. (**D**) Scope of ^{11}C-trifluoromethylation of alkyl iodides. Radiochemical yields are based on the collection of the corresponding product radiochromatogram peaks from the analytical HPLC and are reported as decay-corrected isolated yields from starting activity at the end of [^{11}C]fluoroform production. DMSO, dimethyl sulfoxide; Ph, phenyl.

products were formed in the absence of either the copper(I) catalyst or diazonium salt. Notably, the reaction was complete within 20 min upon the addition of the diazonium salt, meeting the requirement for the translation to radiolabeling. The generality of this aryl-radical–enabled catalytic approach was demonstrated by the late-stage trifluoromethylation of an array of pharmacologically relevant molecules, including derivatives of ospemifene (**3**) and indomethacin (**4**) (see fig. S171 for additional substrates).

More importantly, fluoroform, which can be labeled with either carbon-11 (*53*) or fluorine-18 (*54*, *55*), can also serve as the CF_3 source for this trifluoromethylation pathway (Fig. 2B). Stoichiometric experiments using one equivalent of fluoroform-derived Cu^I–CF_3 with an alkyl iodide **5** revealed that the CF_3 groups could be efficiently transferred to aliphatic sites via the diazonium-promoted pathway. These results are consistent with the single-electron transfer from Cu^I–CF_3 species to the diazonium salt, resulting in the formation of a [Cu^{II}–CF_3] intermediate and an aryl radical (Fig. 2C). The latter expeditiously abstracts an iodine atom from an alkyl iodide substrate, generating an open-shell alkyl radical intermediate. This transient species then readily engages with the [Cu^{II}–CF_3] species, forming trifluoromethylated product, likely through the reductive elimination from a Cu^{III} intermediate (*50*, *56*).

^{11}C-Trifluoromethylation of alkyl iodides

Having established the viability of the aryl-radical–enabled CF_3 transfer, we next sought to translate this approach to ^{11}C-trifluoromethylation. [^{11}C]Fluoroform is readily obtainable from cyclotron-produced [^{11}C]methane by passage over heated cobalt(III) fluoride (*53*). Treatment of [^{11}C]fluoroform with CuBr and potassium *tert*-butoxide (KO^tBu) in *N*,*N*-dimethylformamide (DMF) generates the reactive [^{11}C]$CuCF_3$ species (*53*). The key challenge associated with the translation is the short half-life of carbon-11, which necessitates a rapid reaction between the alkyl iodide, diazonium salt, and [^{11}C]$CuCF_3$. To our satisfaction, under aryl-radical–enabled conditions, [^{11}C]CF_3 groups were efficiently transferred from the copper center into alkyl iodides (Fig. 3A). The labeling was performed by simply adding a solution of diazonium salt and alkyl iodide to a solution of [^{11}C]fluoroform-derived [^{11}C]$CuCF_3$ in DMF. Conducting the experiment with 0.2 to 0.4 gigabecquerel (GBq) of [^{11}C]fluoroform for 10 min at 50°C with precursor alkyl iodide **1** followed by high-performance liquid chromatography (HPLC) purification afforded the labeled compound [^{11}C]**2** after 25 min in 47% ($n = 3$ replicates) yield.

The generality of this ^{11}C-trifluoromethylation reaction was then investigated. Secondary alkyl iodides at cyclic or acyclic positions, along with primary alkyl iodides, were efficiently labeled, affording [^{11}C]**7**–[^{11}C]**11** in 13 to 46% yields. This method was further applied to alkyl iodides derived from medicinally relevant molecules. Sensitive functional groups such as the alkyl chloride in ospemifene [^{11}C]**3**, the lactone in mycophenolic acid [^{11}C]**12**, and tertiary amines in nadifloxacin [^{11}C]**13** and chlorambucil [^{11}C]**14** did not interfere with labeling. A variety of heterocycles are compatible with this protocol, including oxazole in oxaprozin [^{11}C]**15**, indole in indomethacin [^{11}C]**4**, and tadalafil [^{11}C]**16,** as well as pyridine and tetrazole in tedizolid [^{11}C]**17** (44 to 54% yields). Notably, the compatibility with multiple unprotected hydroxyl groups in dapagliflozin ([^{11}C]**18**, 27% yield), which are typically problematic for ^{18}F-fluorination reactions, further highlights the mild and versatile nature of this protocol.

^{18}F-Trifluoromethylation of alkyl iodides

Next, we aimed to apply this aryl-radical–enabled strategy to the ^{18}F-trifluoromethylation reaction. [^{18}F]Fluoroform was readily synthesized from [^{18}F]fluoromethane with minimal molar activity dilution (*54*) or from the reaction of difluoroiodomethane with [^{18}F]fluoride (*55*). The resulting [^{18}F]fluoroform was then converted into [^{18}F]$CuCF_3$ with CuBr and KO^tBu. To our satisfaction, under conditions nearly identical to those for ^{11}C-trifluoromethylation, alkyl iodide **1** reacted efficiently with [^{18}F]fluoroform-derived [^{18}F]$CuCF_3$, affording the ^{18}F-trifluoromethylated product [^{18}F]**2** in 47% yield (Fig. 3A), a yield almost identical to that for [^{11}C]**2**. We then explored the substrate scope of this ^{18}F-trifluoromethylation reaction. A variety of alkyl iodides that were amenable to the ^{11}C-trifluoromethylation protocol underwent efficient ^{18}F-trifluoromethylation, yielding labeled products ([^{18}F]**3**, [^{18}F]**4**, [^{18}F]**11**, and [^{18}F]**12**) in comparable yields (44 to 50%). Additional heterocycles, including thiophene ([^{18}F]**19**) and 4-quinolone ([^{18}F]**20**), were compatible with this protocol (65 and 18% yield). An alkyl iodide bearing an alkyl bromide group was selectively labeled without affecting the alkyl bromide group ([^{18}F]**21**, 39%). In addition, an α-iodoester was also converted into the corresponding radiolabeled product [^{18}F]**22** in useful yield (23%).

Moreover, we applied this protocol to label CF_3 analogs of established pharmaceutical molecules (Fig. 3B). The [^{18}F]CF_3 analogs of STS-135 and O-1269 ([^{18}F]**23** and [^{18}F]**24**), both of which are established cannabinoid receptor (CBR) agonists, were readily synthesized from their alkyl iodide precursors in moderate yields (17 and 40% yield, respectively). Additionally, the CF_3 counterpart of a highly selective CBR ligand derived from 2-hydroxyquinoline [^{18}F]**25** was successfully synthesized (*57*). This strategy was also extended to the radiosynthesis of a CF_3 counterpart of a tumor imaging agent, [^{18}F]**26**, an analog of the clinically used [^{18}F]2-fluoroethyl-L-tyrosine (FET). Given the expected enhancement in metabolic stability conferred by CF_3 groups, [^{18}F]**26** holds the potential for PET imaging applications.

The synthetic utility of this protocol has been further demonstrated by labeling CF_3-containing drug candidates (Fig. 3C). BAY 59-3074, a CF_3-containing CBR partial agonist developed by Bayer AG, was efficiently labeled with fluorine-18 at the CF_3 group, yielding [^{18}F]**27** in 51% yield. Notably, a previous approach for labeling this molecule with fluorine-18 involved sophisticated organometallic synthesis and resulted in considerably lower yield (*41*). Furthermore, we sought to radiolabel IAMA-6, a selective inhibitor of sodium potassium chloride cotransporter 1 (NKCC1) for treating autism and epilepsy (*58*). Gratifyingly, IAMA-6 was efficiently radiolabeled with fluorine-18, either as its methyl ester analog ([^{18}F]**28**, 75% yield) or in its free carboxylic acid form ([^{18}F]**29**, 32% yield).

Finally, this protocol has been successfully applied to the synthesis of a long-sought-after monoamine oxidase B (MAO-B) radioligand, [^{18}F]**SL25.1188** (Fig. 3D). Its carbon-11 counterpart, [^{11}C]**SL25.1188**, labeled with carbon-11 at the carbonyl position, is known to be an excellent PET tracer for imaging MAO-B in the human brain (*59*, *60*). Despite the presence of a CF_3 group in this molecule, all previous efforts to label with fluorine-18 have failed owing to the lack of a viable ^{18}F-trifluoromethylation strategy, whereas the simple ^{18}F-labeled monofluoro analog suffers from undesirable in vivo radiodefluorination (*61*, *62*). To our satisfaction, the CF_3 group of **SL25.1188** can be efficiently radiolabeled with fluorine-18 from its alkyl iodide precursor, affording [^{18}F]**30** in 55% yield (115 MBq isolated). These examples further highlight the potential of this method to overcome long-standing challenges in PET tracer development.

Decarboxylative ^{11}C- and ^{18}F-trifluoromethylation of alkyl carboxylic acids

Having demonstrated that copper could mediate radiotrifluoromethylation of alkyl radicals generated in situ, we sought to extend this radiotrifluoromethylation pathway to other alkyl radical precursors beyond alkyl iodides. Early studies from our group revealed that *N*-hydroxyphthalimide (NHP) esters, derived from alkyl carboxylic acids, could undergo efficient decarboxylative difluoromethylation reactions (*44*). These prior results prompted us to explore a decarboxylative radiotrifluoromethylation strategy under Cu-mediated conditions. Initially, treating NHP esters with fluoroform-derived Cu–CF_3 did not yield desired products. Interestingly, the decarboxylative trifluoromethylation reactions proceeded smoothly under blue-light irradiation using a ruthenium photocatalyst, $Ru(bpy)_3Cl_2 \cdot 6H_2O$, where bpy is 2,2′-bipyridine (Fig. 4A). NHP esters derived from both primary and secondary carboxylic acids could be converted into the desired products (**31** and **32**; see fig. S142 for additional substrates). Mechanistically, we reason that the oxidation of Cu^I–CF_3 by the excited state of the photocatalyst generates a [Cu^{II}–CF_3] intermediate. Concurrently, the NHP ester undergoes single-electron reduction by the reduced state of the photocatalyst, forming an alkyl radical intermediate, which couples with [Cu^{II}–CF_3] to deliver the trifluoromethylated product.

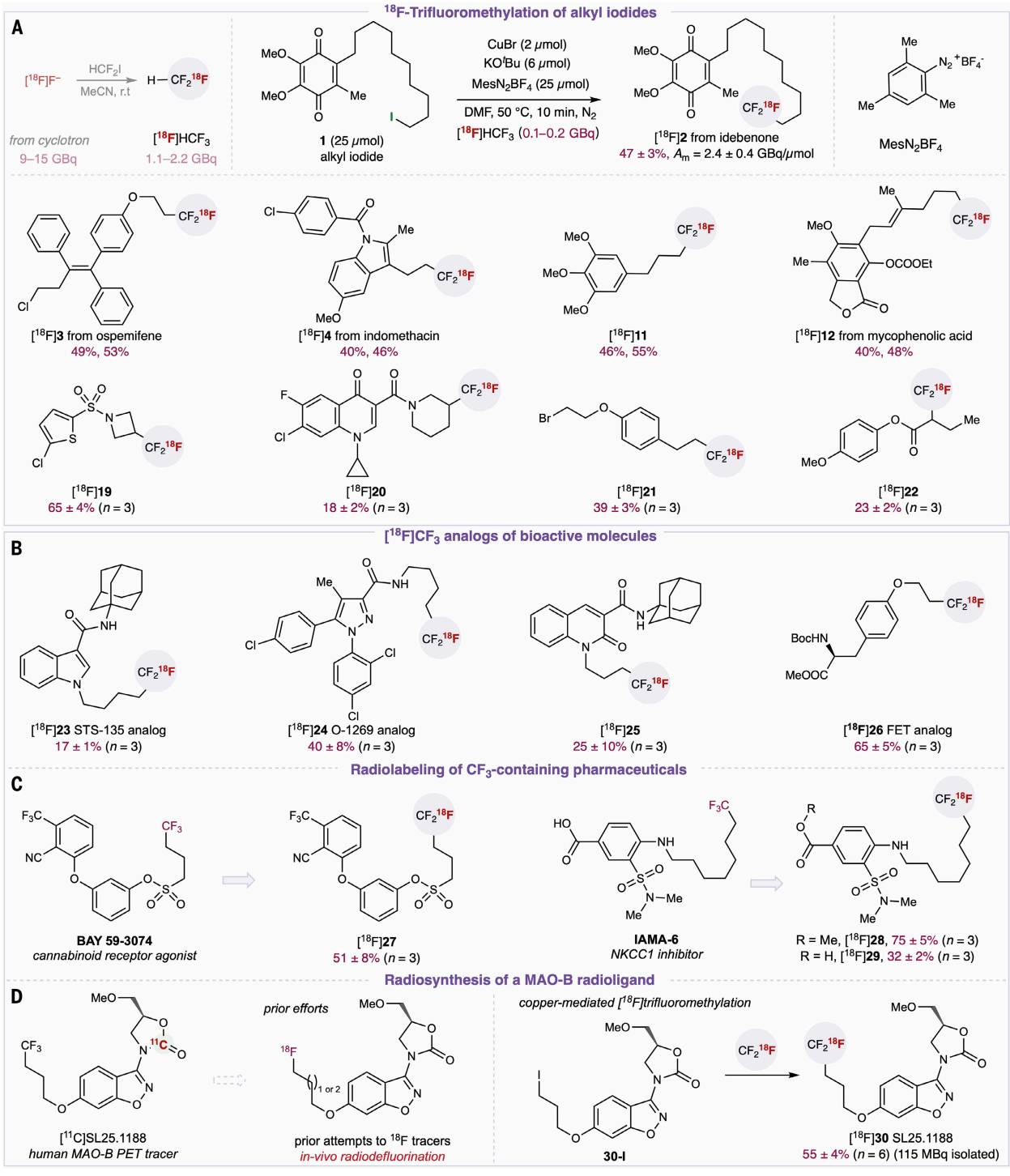

Fig. 3. Scope of ^{18}F-trifluoromethylation of alkyl iodides. (**A**) Development of [^{18}F]-trifluoromethylation of alkyl iodides. (**B**) Synthesis of [^{18}F]CF_3 analogs of bioactive molecules. (**C**) Radiolabeling of CF_3-containing pharmaceuticals. (**D**) Radiosynthesis of an MAO-B radioligand. Radiochemical yields are based on the collection of the corresponding product radiochromatogram peaks from the analytical HPLC and are reported as decay-corrected isolated yields from starting activity at the end of [^{18}F]fluoroform production. Individual results are reported for $n = 2$ replicates, and means ± SD are reported for $n \geq 3$ replicates. Molar activity corrected at the end of radionuclide production is shown. Boc, *tert*-butyloxycarbonyl.

Notably, this transformation was complete within a short time (< 2 hours), making it suitable for translation to radiolabeling reactions.

Encouraged by this photoredox-catalyzed decarboxylative trifluoromethylation, we turned our attention to radiolabeling with carbon-11 and fluorine-18. Gratifyingly, using either [^{11}C]fluoroform or [^{18}F]fluoroform as the CF_3 source, the NHP ester ***33*** underwent efficient decarboxylative ^{11}C- and ^{18}F-trifluoromethylation under Cu-mediated photoredox conditions, affording [^{11}C]***31*** and [^{18}F]***31*** in 39 and 67% yield, respectively, within 10 min (Fig. 4B). We then explored the substrate scope of this decarboxylative radiotrifluoromethylation reaction. A group of NHP esters derived from primary and secondary carboxylic acids underwent efficient decarboxylative ^{11}C- and ^{18}F-trifluoromethylation:

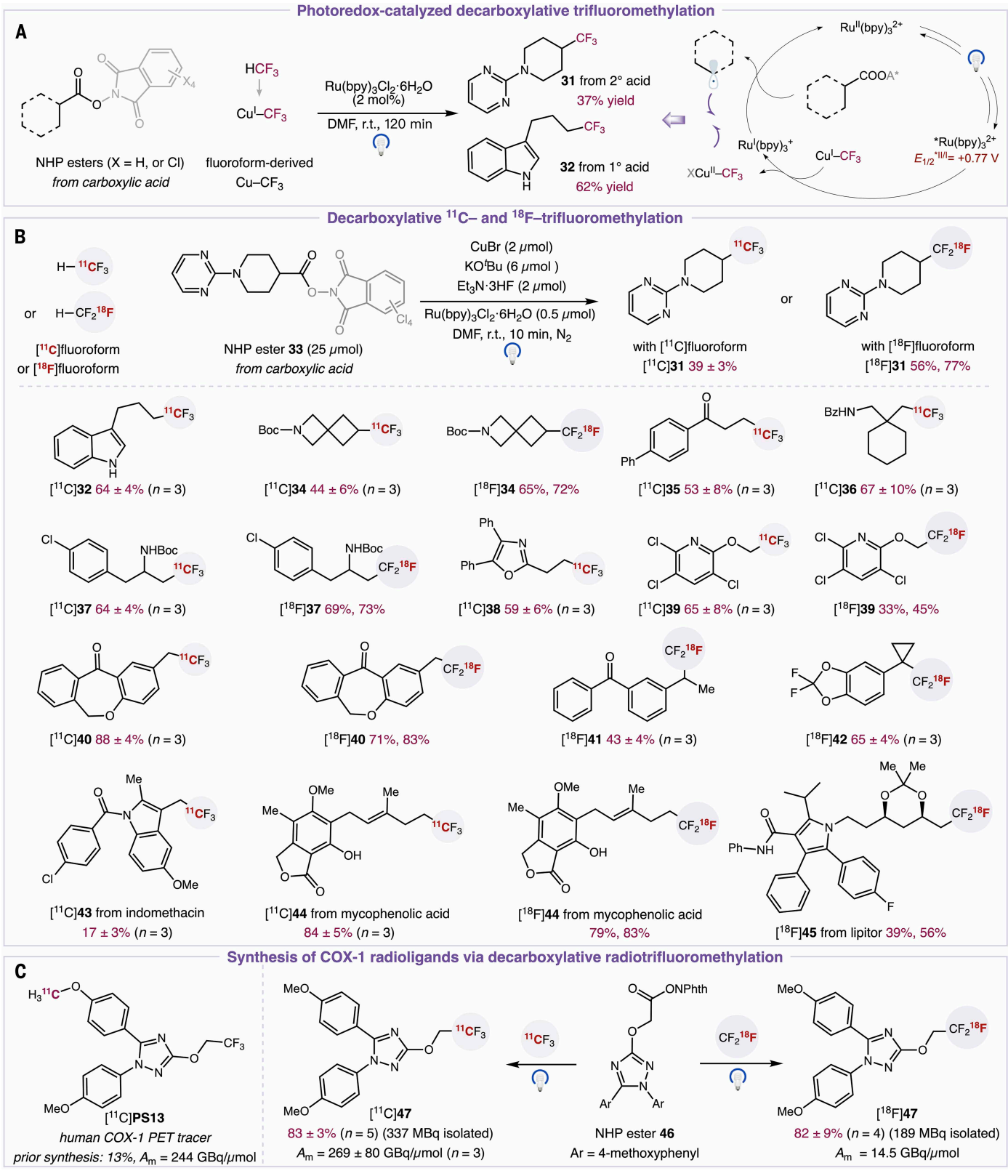

Fig. 4. Decarboxylative ^{11}C- and ^{18}F-trifluoromethylation of alkyl carboxylic acids. (**A**) Development of a photoredox-catalyzed decarboxylative trifluoromethylation reaction. (**B**) Scope of ^{11}C- and ^{18}F-decarboxylative trifluoromethylation. (**C**) Radiosynthesis of COX-1 radioligands, [^{11}C]**PS13** and [^{18}F]**PS13**. Radiochemical yields are based on the collection of the corresponding product radiochromatogram peaks from the analytical HPLC and are reported as decay-corrected isolated yields from starting activity at the end of [^{11}C]fluoroform or [^{18}F]fluoroform production. Individual results are reported for $n = 2$ replicates, and means ± SD are reported for $n \geq 3$ replicates. Molar activity (A_m) corrected at end of radionuclide production. Bz, benzoyl; $E_{1/2}$, reduction potential versus saturated calomel electrode; Phth, phthaloyl; r.t., room temperature.

[^{11}C]**32**, [^{11}C]/[^{18}F]**34**, [^{11}C]**35**, [^{11}C]**36**, [^{11}C]/[^{18}F]**37**, and [^{11}C]**38** (44 to 71% yields). Notably, NHP esters derived from an aryloxy acetic acid ([^{11}C]/[^{18}F]**39**), as well as from primary ([^{11}C]/[^{18}F]**40**), secondary ([^{18}F]**41**), and tertiary ([^{18}F]**42**) benzylic carboxylic acids, underwent efficient decarboxylation reactions, delivering radiolabeled products in 39 to 88% yield. These results highlight the utility of this approach as a complementary method to the aryl-radical–enabled protocol, particularly for cases where corresponding alkyl iodides are often unstable. Pharmaceutical compounds, such as indomethacin, mycophenolic acid, and lipitor, were successfully converted into their radiolabeled products—[^{11}C]**43**, [^{11}C]/[^{18}F]**44**, and [^{18}F]**45**, respectively—in moderate to good yields (17 to 84%).

Finally, we applied this decarboxylative radiotrifluoromethylation reaction to the synthesis of PET radioligands for imaging cyclooxygenase subtype 1 (COX-1) (Fig. 4C). [^{11}C]**PS13**, developed by one of our groups, is a highly effective COX-1 radioligand used for PET imaging in the human brain (*43*). However, previous attempts to label the CF_3 group of **PS13** with fluorine-18 resulted in poor radiochemical yield (*35*). To our satisfaction, under our standard decarboxylative radiotrifluoromethylation conditions, NHP ester **46** was efficiently converted into [^{11}C]**47** and [^{18}F]**47** in high yield (83 and 82%, respectively, with up to 337 MBq isolated, at the end of synthesis). Measuring the molar activity of the labeled products revealed that [^{11}C]**47** was formed with a high molar activity (A_m = 269 GBq/μmol), whereas [^{18}F]**47** exhibited a molar activity comparable to that of [^{18}F]fluoroform (A_m = 14.5 GBq/μmol). Because the synthesis of [^{18}F]fluoroform with higher molar activity (>30 GBq/μmol) has been reported (*55*, *63*), we anticipate that [^{18}F]CF_3-labeled products with higher molar activity can be readily accessed when high-A_m imaging studies are required. Finally, an automated apparatus was developed for this photochemical radiolabeling reaction, enabling the radiosynthesis of [^{11}C]**PS13** in 65% yield. Overall, these results further underscore the potential of our methods for synthesizing hitherto challenging PET radioligands.

Given the broad scope and operational simplicity of these radiolabeling reactions, we anticipate their wide range of applications in the field of PET imaging. Moreover, the demonstration that radiolabeled CF_3 groups can be readily transferred to alkyl radical intermediates opens an avenue for developing previously inaccessible ^{11}C- and ^{18}F-labeled compounds.

REFERENCES AND NOTES

1. M. E. Phelps, *Proc. Natl. Acad. Sci. U.S.A.* **97**, 9226–9233 (2000).
2. S. R. Cherry *et al.*, *Sci. Transl. Med.* **9**, eaaf6169 (2017).
3. J. K. Willmann, N. van Bruggen, L. M. Dinkelborg, S. S. Gambhir, *Nat. Rev. Drug Discov.* **7**, 591–607 (2008).
4. S. M. Ametamey, M. Honer, P. A. Schubiger, *Chem. Rev.* **108**, 1501–1516 (2008).
5. X. Deng *et al.*, *Angew. Chem. Int. Ed.* **58**, 2580–2605 (2019).
6. J. Rong, A. Haider, T. E. Jeppesen, L. Josephson, S. H. Liang, *Nat. Commun.* **14**, 3257 (2023).
7. A. Pees, M. Chassé, A. Lindberg, N. Vasdev, *Molecules* **28**, 931 (2023).
8. K. Dahl, C. Halldin, M. Schou, *Clin. Transl. Imaging* **5**, 275–289 (2017).
9. P. J. H. Scott, *Angew. Chem. Int. Ed.* **48**, 6001–6004 (2009).
10. J. B. I. Sap *et al.*, *Nature* **606**, 102–108 (2022).
11. R. W. Pipal *et al.*, *Nature* **589**, 542–547 (2021).
12. S. Preshlock, M. Tredwell, V. Gouverneur, *Chem. Rev.* **116**, 719–766 (2016).
13. M. Zhang, S. Li, H. Zhang, H. Xu, *Eur. J. Med. Chem.* **205**, 112629 (2020).
14. O. Jacobson, D. O. Kiesewetter, X. Chen, *Bioconjug. Chem.* **26**, 1–18 (2015).
15. J. Ajenjo, G. Destro, B. Cornelissen, V. Gouverneur, *EJNMMI Radiopharm. Chem.* **6**, 33 (2021).
16. R. Littich, P. J. H. Scott, *Angew. Chem. Int. Ed.* **51**, 1106–1109 (2012).
17. E. L. Cole, M. N. Stewart, R. Littich, R. Hoareau, P. J. Scott, *Curr. Top. Med. Chem.* **14**, 875–900 (2014).
18. A. F. Brooks, J. J. Topczewski, N. Ichiishi, M. S. Sanford, P. J. H. Scott, *Chem. Sci.* **5**, 4545–4553 (2014).
19. P. Mishra, J. Hind, I. A. Fallis, M. Tredwell, *Org. Lett.* **27**, 1724–1728 (2025).
20. E. Lee *et al.*, *Science* **334**, 639–642 (2011).
21. V. W. Pike, in *Molecular Imaging of Neurodegenerative Disorders*, D. J. Cross, K. Mosci, S. Minoshima, Eds. (Springer, 2023), pp. 35–55.
22. F. Wuest, M. Berndt, T. Kniess, in *PET Chemistry: The Driving Force in Molecular Imaging*, vol. 64, Ernst Schering Foundation Symposium Proceedings Series, F. Wuest, M. Berndt, T. Kneiss, Eds. (Springer, 2007), pp. 183–213.
23. A. S. Nair *et al.*, *Processes* **10**, 2054 (2022).
24. B. K. Park, N. R. Kitteringham, *Drug Metab. Rev.* **26**, 605–643 (1994).
25. H. J. Böhm *et al.*, *Chembiochem* **5**, 637–643 (2004).
26. S. Purser, P. R. Moore, S. Swallow, V. Gouverneur, *Chem. Soc. Rev.* **37**, 320–330 (2008).
27. V. W. Pike, *Trends Pharmacol. Sci.* **30**, 431–440 (2009).
28. M. Kuchar, C. Mamat, *Molecules* **20**, 16186–16220 (2015).
29. M. Huiban *et al.*, *Nat. Chem.* **5**, 941–944 (2013).
30. L. Veth, A. D. Windhorst, D. J. Vugts, *Angew. Chem. Int. Ed.* **64**, e202416901 (2025).
31. S. Jana, S. Telu, J. E. Jakobsson, B. Y. Yang, V. W. Pike, *Chem. Commun.* **60**, 4589–4592 (2024).
32. Q. Zhao, S. Telu, S. Jana, C. L. Morse, V. W. Pike, *Nat. Commun.* **15**, 5798 (2024).
33. M. V. Fawaz *et al.*, *ACS Chem. Neurosci.* **5**, 718–730 (2014).
34. V. T. Lien, P. J. Riss, *BioMed Res. Int.* **2014**, 380124 (2014).
35. C. Taddei *et al.*, *ACS Chem. Neurosci.* **12**, 517–530 (2021).
36. V. Kramer *et al.*, *ACS Chem. Neurosci.* **11**, 427–435 (2020).
37. W. Rafique *et al.*, *ACS Omega* **3**, 7567–7579 (2018).
38. P. J. Riss *et al.*, *Org. Biomol. Chem.* **10**, 6980–6986 (2012).
39. P. J. Riss, F. I. Aigbirhio, *Chem. Commun.* **47**, 11873–11875 (2011).
40. F. Francis, F. Wuest, *Molecules* **26**, 6478 (2021).
41. M. D. Levin *et al.*, *Science* **356**, 1272–1276 (2017).
42. W. Saba *et al.*, *Synapse* **64**, 61–69 (2010).
43. S. Shrestha *et al.*, *ACS Chem. Neurosci.* **9**, 2620–2627 (2018).
44. X. Zeng *et al.*, *J. Am. Chem. Soc.* **141**, 11398–11403 (2019).
45. D. J. P. Kornfilt, D. W. C. MacMillan, *J. Am. Chem. Soc.* **141**, 6853–6858 (2019).
46. H. Xiao *et al.*, *Chem* **5**, 940–949 (2019).
47. X. Zhao, D. W. C. MacMillan, *J. Am. Chem. Soc.* **142**, 19480–19486 (2020).
48. H. Shen *et al.*, *J. Am. Chem. Soc.* **139**, 9843–9846 (2017).
49. A. Cai, W. Yan, C. Wang, W. Liu, *Angew. Chem. Int. Ed.* **60**, 27070–27077 (2021).
50. W. Yan *et al.*, *J. Am. Chem. Soc.* **146**, 15176–15185 (2024).
51. L. Caiger, H. Zhao, T. Constantin, J. J. Douglas, D. Leonori, *ACS Catal.* **13**, 4985–4991 (2023).
52. X.-Y. Lv, R. Martin, *Org. Lett.* **25**, 3750–3754 (2023).
53. M. B. Haskali, V. W. Pike, *Chemistry* **23**, 8156–8160 (2017).
54. B. Y. Yang, S. Telu, M. B. Haskali, C. L. Morse, V. W. Pike, *Sci. Rep.* **9**, 14835 (2019).
55. D. van der Born *et al.*, *Angew. Chem. Int. Ed.* **53**, 11046–11050 (2014).
56. Y. Luo *et al.*, *Science* **381**, 1072–1079 (2023).
57. S. Pasquini *et al.*, *J. Med. Chem.* **54**, 5444–5453 (2011).
58. M. Borgogno *et al.*, *J. Med. Chem.* **64**, 10203–10229 (2021).
59. S. Moriguchi *et al.*, *JAMA Psychiatry* **76**, 634–641 (2019).
60. V. Narayanaswami *et al.*, *ACS Chem. Neurosci.* **10**, 1867–1871 (2019).
61. J. W. Hicks *et al.*, *Bioorg. Med. Chem. Lett.* **25**, 288–291 (2015).
62. K. Dahl *et al.*, *Bioorg. Med. Chem. Lett.* **29**, 1624–1627 (2019).
63. A. Pees *et al.*, *J. Labelled Comp. Radiopharm.* **64**, 466–476 (2021).
64. J. Hong, Source code for instrumentation for trifluoromethylation. Zenodo (2025); https://doi.org/10.5281/zenodo.17428392.

ACKNOWLEDGMENTS

The authors thank the NIH Clinical Center (P. Herscovitch) for radioisotope production. **Funding:** This work was supported by the National Institute of General Medical Sciences (R35GM146765 to W.L.), the National Institute of Biomedical Imaging and Bioengineering (R01EB036046 to W.L.), and the Intramural Research Program of the NIH, National Institute of Mental Health (NIMH) (ZIA-MH002793 to V.W.P.). The contributions of the NIH authors are considered works of the US government. The findings and conclusions presented in this paper are those of the authors and do not necessarily reflect the views of the NIH or the US Department of Health and Human Services. NMR experiments at the University of Cincinnati were performed using a Bruker AVANCE NEO 400 MHz NMR spectrometer, funded by NSF-MRI grant CHE-1726092. **Author contributions:** Conceptualization: W.L., V.W.P.; Methodology: W.L., V.W.P., C.W., P.D., S.J., J.H.; Investigation: C.W., P.D., S.J., J.H.; Funding acquisition: W.L., V.W.P.; Project administration: W.L., V.W.P.; Supervision: W.L., V.W.P.; Writing – original draft: W.L., V.W.P.; Writing – review & editing: W.L., V.W.P., C.W., P.D., S.J., J.H. **Competing interests:** The authors declare that they have no competing interests. **Data and materials availability:** Details for the synthesis of all chemical compounds reported here are given in the methods section of the supplementary materials. All characterization data are in supplementary materials. LabVIEW scripts for automated radiotrifluoromethylation have been deposited at Zenodo (*64*).

SUPPLEMENTARY MATERIALS

science.org/doi/10.1126/science.ady2969
Materials and Methods; Supplementary Text; Figs. S1 to S174; Tables S1 to S13; HPLC Traces; NMR Spectra; References (*65*–*84*)

Submitted 29 April 2025; accepted 28 October 2025

10.1126/science.ady2969